Preprints of the 19th World Congress
The International Federation of Automatic Control
Cape Town, South Africa. August 24-29, 2014

Analysis of On/Off Controllers of a Semi-Active Suspension in a CAN

Alexandro A. Ortiz Espinoza, * **Alan M. Cabello Ortega,** *
Juan Carlos Tudon-Martinez * **Diana Hernández-Alcantara** *
and Ruben Morales-Menendez *

* *Tecnológico de Monterrey, Monterrey NL, México, {A00787745, A00393940, A00287756, A00469139, rmm }@itesm.mx*

Abstract: A performance analysis of automotive semi-active suspension control algorithms was realized. Three *on/off* control strategies were tested in a quarter of vehicle model: *hybrid Sky Hook-Ground Hook*, *hybrid Mix-1-Sensor* and *Frequency Estimation-Based* controller. A commercial *Magneto-Rheological* damper was modeled by using an *Artificial Neural Network* approach. The automotive semi-active suspension was implemented in a commercial *Controller Area Network* system; and the control algorithms were implemented in a micro-controller system with comfort and road holding as main goals. Early results show the feasibility of this application.

Keywords: Automotive Semi-Active suspension, CAN, Ride comfort, Road holding

1. INTRODUCTION

The main goal of automotive suspension system is to isolate the vehicle chassis from road disturbances (comfort) as well as to keep in contact the wheel and the road (road holding). These objectives could be performed simultaneously in a semiactive suspension systems by modifying some parameters of the damper, [Sankaranarayanan et al., 2008]. However, this demands an automatic control system. Even the design of controllers for semi-active suspensions has been widely studied in the automotive control domain, there are several opportunities if they are implemented in a *Networked Control System* (*NCS*). One of the disadvantages of *NCS* is the introduction of a time delay in different forms between sensors, controllers and actuators. The time delay is induced from time sharing of the network and the extra time needed for physical signal coding and communication processing, Vargas-Rodriguez and Morales-Menendez [2007].

In order to study the feasibility of a semiactive control system implementation, an experimental platform using *NCS* environment was developed; the *Quarter of Vehicle QoV* model and damper model were embedded in a *cRIO* of *National Instruments*^{TM} to mimic the suspension behavior in real-time, a micro-controller *Arduino Due* hosts the control algorithms. Different control algorithms under several tests and network traffic load were considered to evaluate the approach.

This paper is organized as follows: in section 2, some issues of *NCS* and the *Controller Area Network* (*CAN*) are introduced. Section 3 presents the implemented vehicle suspension model. The experimental damper model is shown in section 4. Section 5 describes the developed experimental set up. Section 6 discusses the results; and finally, section 7 concludes this paper.

2. CONTROLLER AREA NETWORK

Control networks can replace point-to-point wired systems providing several advantages. They can reduce the volume of wiring and the points of failure while they enhance the capability of troubleshooting/maintenance, the devices inter-operability and the reconfigurability of the control systems. In addition, the use of control networks allows the implementation of intelligent distributed control systems, Marshall [2001].

When a network is used in an automatic control system, the performance depends not only on the quality of service of the network, but also on how the network is used. Using a common-bus instead of point-to-point approach, introduces different forms of time delay uncertainty between sensors, actuators, and controllers. These time delays come from the time sharing of communication medium as well as additional functionality required for physical signal coding and communication processing. The characteristics of time delays could be constant, bounded, or even random, depending on the network protocols. Time delay could drastically reduce the performance, Lian et al. [2005].

Figure 1 presents how the control performance changes with the sampling period for continuous, digital and networked control systems. The performance of the continuous control system is independent of the sampling time. The worst, unacceptable, acceptable, and best regions can be defined based on control system specifications. The performance axis could be chosen to reflect a subset of these metrics. The digital control system performance depends on the sampling time, if the sampling time is smaller the performance converges to the continuous control system approach. The *NCS* performance is worse than the digital control system at low frequencies, because to the extra

⋆ This work was supported by *CONACyT* (Bilateral project México-Spain 142183) and *Tecnológico de Monterrey* (Autotronics Research Chair). Authors thank *METALSA* for sharing its experimental setup

delay associated with the network. Another important issue is a saturated network if the sampling frequency is increased. The optimized sample period must be between the extreme of control and networking requirements, Lian et al. [2002].

The selection of the best sampling period is a trade off on the performance computation of points A, B and C in Fig. 1. The performance point A of sampling period P_A in digital control could be estimated based on the relationship between control system bandwidth and sampling rate. For the *NCS*, point B of sampling period P_B can be found by investigating the characteristics and statistics of network-induced delays and device computing time delays. As the sampling period decreases, the network traffic load grows up, the possibility of more contention time or data loss increases in a bandwidth-limited network and longer time delays result then the point C, Lian et al. [2002].

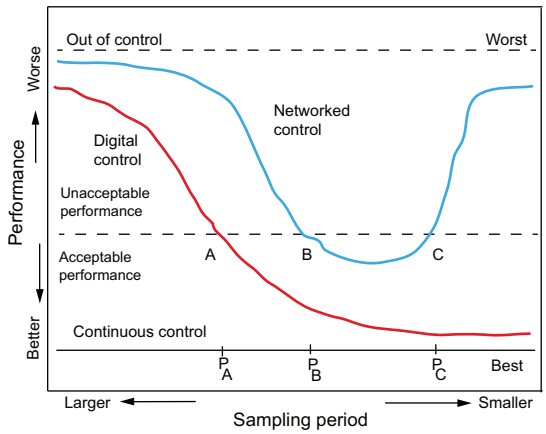

Fig. 1. Performance comparison of continuous, digital and networked control systems, Lian et al. [2002].

The *Society of Automotive Engineers* (*SAE*) divides vehicular network protocol into 4 classes: A, B, C and D based on data transmission speed. Class A network has a data transmission speed lower than 10 kbps and it is used to transmit simple control data. Local Interconnect Network is the typical example of class A network. Class B network has a speed from 10 kbps to 125 kbps and it is used for data exchange between *Electronic Control Units* (*ECUs*) to reduce the length of wiring and the number of sensors by sharing data. Low-speed *Controller Area Network* (*CAN*), it is the typical representation of class B. Class C network applies in high speed communications and real-time control with speed of 125 kbps $\sim$ 1 Mbps. High-speed *CAN* and *SAE J1939*, SAE [2005], are typical class C network protocols and are used for the Engine Electronic Control System and chassis domain. Class D network has a speed over 1 Mbps and be also used for real-time communication and control.

The majority of automobile manufacturers evolved and adopted for the general purpose communication the *CAN* standard, Hu et al. [2007]. The *CAN* is a serial bus communications protocol developed in the early 1980s, R. Bosch GmbH [1991]. It defines a standard for communication between sensor, actuator, controller, and other nodes in realtime applications. The *CAN* protocol standardizes the physical and data link layers, which are the two lowest layers of the Open Systems Interconnection communication model. The communication rate of a network based on *CAN* depends on the physical distances between the nodes. It can be 1 Mbps for less than 40 m.

CAN protocol only comprise physical and data link layers, not application layer. The application layer protocol can be self-defined, or a standard protocol of international organization such as *CANOpen* or *SAE J1939* is chosen for the specific system. The goal of the *CAN* application layer protocol is to maximize the real-time performance of *CAN* bus, and reduce network load rate.

The comfort and road holding control system were implemented in an *Axiomatic*^{TM} *CAN* system to evaluate the performance on a *NCS*.

3. AUTOMOTIVE SEMIACTIVE SUSPENSION

According to the capability to adjust the damping force, the automotive suspensions can be classified as: passive, active or semi-active. Passive suspensions consist on a spring used to store energy for some time interval of a suspension cycle in parallel with a passive shock absorber used to dissipate it. Active suspensions are able to store, dissipate and generate energy to control the chassis motion by using a fully active actuator in parallel with a spring; an external power supply is needed. Semi-active control suspension provides similar performances of active actuators without requiring a significant external power supply.

The semi-active suspensions consist on a spring and damping component; its continuous variable damping coefficient can be adjusted by external control signals. There are 4 main types of semi-active dampers in the market: electro-hydraulic, pneumatic, magneto-rheological, and electro-rheological.

Even a full vehicle model was implemented in the *Axiomatic*^{TM} *CAN* system, an automotive semiactive suspension can be studied by a lumped parameter single corner model, better known as a *Quarter of Vehicle* (*QoV*) model,Fig. 2A. The (*QoV*) model describes the sprung mass (m_s) corresponding to the vehicle chassis and components supported by the suspension, and the unsprung mass (m_{us}); this model only captures vertical motions. The tire is modelled by a spring linked to the road (z_r) and represented with a stiffness coefficient (k_t) while the tire damping is negligible. A contact point between the road and the tire is always assumed. The suspension deflection is $z_{def} = z_s - z_{us}$. The parameters of the *QoV* model are computed assuming a uniform distribution of the weight (two front passengers and mid-level fuel tank).

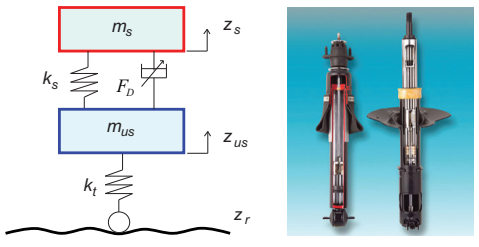

(A) Quarter of Vehicle (QoV) model (B) Delphi MagneRide^{TM}damper

Fig. 2. *QoV* model and *Delphi MagneRide*^{TM} damper

The dynamic model is:

$$\begin{aligned} m_s\ddot{z}_s &= -F_D - k_s z_{def} \\ m_{us}\ddot{z}_{us} &= k_s z_{def} + F_D - k_t(z_{us} - z_r) \end{aligned} \tag{1}$$

and the state-space representation is:

$$\underbrace{\begin{bmatrix} \ddot{z}_s \\ \dot{z}_s \\ \ddot{z}_{us} \\ \dot{z}_{us} \end{bmatrix}}_{\dot{x}} = \underbrace{\begin{bmatrix} 0 & -\frac{k_s}{m_s} & 0 & \frac{k_s}{m_s} \\ 1 & 0 & 0 & 0 \\ 0 & \frac{k_s}{m_{us}} & 0 & -\frac{k_s+k_t}{m_{us}} \\ 0 & 0 & 1 & 0 \end{bmatrix}}_{A} \underbrace{\begin{bmatrix} \dot{z}_s \\ z_s \\ \dot{z}_{us} \\ z_{us} \end{bmatrix}}_{x} + \underbrace{\begin{bmatrix} -\frac{1}{m_s} & 0 \\ 0 & 0 \\ \frac{1}{m_{us}} & \frac{k_t}{m_{us}} \\ 0 & 0 \end{bmatrix}}_{B} \underbrace{\begin{bmatrix} F_D \\ z_r \end{bmatrix}}_{u}$$

$$\underbrace{\begin{bmatrix} z_{def} \\ \dot{z}_s \\ \dot{z}_{us} \\ \ddot{z}_s \\ \ddot{z}_{us} \end{bmatrix}}_{y} = \underbrace{\begin{bmatrix} 0 & 1 & 0 & -1 \\ 1 & 0 & 0 & 0 \\ 0 & 0 & 1 & 0 \\ 0 & -\frac{k_s}{m_s} & 0 & \frac{k_s}{m_s} \\ 0 & \frac{k_s}{m_{us}} & 0 & -\frac{k_s+k_t}{m_{us}} \end{bmatrix}}_{C} \begin{bmatrix} x \end{bmatrix} + \underbrace{\begin{bmatrix} 0 & 0 \\ 0 & 0 \\ 0 & 0 \\ -\frac{1}{m_s} & 0 \\ \frac{1}{m_{us}} & \frac{k_t}{m_{us}} \end{bmatrix}}_{D} \begin{bmatrix} u \end{bmatrix} \tag{2}$$

where $\ddot{z}_s$, $\dot{z}_s$ and z_s are the acceleration, velocity and position of the sprung mass; $\ddot{z}_{us}$, $\dot{z}_{us}$ and z_{us} are for the unsprung mass. For a better representation of the semiactive suspension system an experimental damper model will be considered to mimic the damper force, F_D.

4. ANN-BASED MR DAMPER MODELING

A commercial damper, manufactured by *Delphi MagneRide*™ was used in this research, Fig. 2B. It has continuous actuation and considerable hysteresis at high frequencies with high deflections. Its range of force is 4,000 N, with 40 mm of stroke and time constant of 15 ms. This damper exploits the physical properties of *Magneto-Rheological MR* fluids. They change their viscosity when subject to a magnetic field field. An *MR* fluid consists of a mixture of oil and micro-particles sensitive to the magnetic field. This fluid becomes very viscous when a magnetic field is applied; otherwise, it behaves as a liquid when no field is applied.

Since the *MR* damper is the key element in the semiactive suspension system, an accurate experimental model is needed.

Two major groups have been established in the *MR* damper modeling: parametric and non-parametric structures. The parametric models describe the physical phenomena in mathematical expressions. The non-parametric models represent this device without considering an *a priori* knowledge; the coefficients do not have a physical meaning, such as the *Artificial Neural Network* (*ANN*) approach. The main advantages of the *ANN*-based modeling is the simplicity of structure, extrapolation capability, simple identification algorithm and low number of parameters.

Two major groups of *ANN* have been considered according to the flow of signals into the architecture. *Feedforward* networks project the flow of information only in one way, where a neuron in a layer is fed by the outputs of all neurons of the previous layer; while, *recurrent* networks have an output feedback signal used as an internal memory into the network.

To identify an accurate experimental model, a *Design of Experiments* (*DoE*) was implemented in an industrial laboratory where a *MTS-407*™ controller has been used to control the position of the damper piston. An *NI-9172*™ data acquisition system commands the controller and records the main variables of the *MR* damper. The bandwidth of displacement was 0.5 - 15 Hz, which lies within comfort and road holding automotive applications.

The main goal was to obtain the simplest (but precise) *ANN* architecture that supports its implementation in a semi-active suspension control system. Ten replicas of each experiment were used to evaluate statistically the modeling results; for each replica, 60 % of the data were used in the learning phase and the remainder in the testing phase. The *ANN* architecture (2 input neurons, 10 hidden neurons, 1 output neuron) has been chosen. The proposed *ANN*-based was intensively validated with experimental tests that explore all phenomena of the *MR* damper. Modeling results show that the *ANN* correctly describes the damper behavior with low error (median of 6 % and mean of 7.2 %).

5. EXPERIMENTAL SYSTEM

The architecture of the *CAN* system is shown in Fig. 3. It was implemented with: 4 Analog Input modules *Axiomatic*^{TM} AX030100, 4 Analog Output modules *Axiomatic*^{TM} AX022400, 2 inclinometers *Axiomatic*^{TM} AX06020X and 1 (*Arduino Due*) micro-controller that works as an *ECU*. The bandwidth of the *CAN* bus was 250 kbits/s.

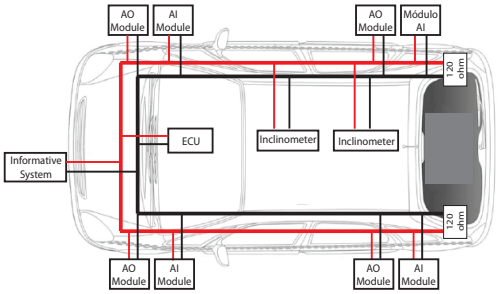

Fig. 3. *CAN* architecture.

The *QoV* model was embedded in *cRio* 9014 of *NI*^{TM} which has two modules: an analog output *NI* 9263 module and digital input *NI* 9401. The signals sent by the analog output module are: $\dot{z}_s$, $\ddot{z}_s$, $\dot{z}_{us}$ and $\ddot{z}_{us}$, which are in the range of 0 – 5 V. The analog input *CAN* module receives these four signals, which are sampled every 10 ms and it samples all inputs every 10 ms. The digital input module receives the *PWM* signal sent by an analog output *CAN* module. The *PWM* signal has a frequency of 20 kHz and a 0 - 100 % duty cycle, Fig. 4.

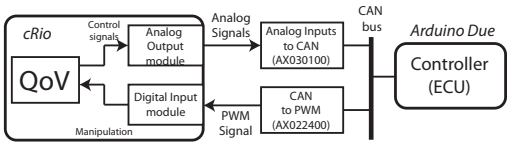

Fig. 4. *QoV* model into the *CAN* system.

The inclinometers were configured to measure three angles: yaw, pitch and roll in range ± 80 grades of experimental vehicle, but they were not used for this project.

The *ECU* was implemented in a micro-controller *Arduino Due* as an embedded control system. Two *Texas Instrument*$^{\text{TM}}$transceivers (one on each port) were used to perform the communication between *ECU* and *CAN*. To access the *Arduino CAN* ports, two libraries were added to the main code.

A data-based controller only needs measurements and analytical estimations to monitor the suspension behavior and to adjust the damping force according to the desired performances. Many semi-active suspension controllers have been proposed for a *QoV* model. Three controllers were implemented in the *ECU* in order to evaluate their feasibility and performance on a *NCS*. First, the hybrid *Sky-Hook and Ground-Hook* (*SH-GHc*) controller oriented to comfort. The *Sky-Hook* algorithm is, Karnopp et al. [1974]:

$$F_{SH} = \begin{cases} c_{SH}\dot{z}_{us} & \text{if } \dot{z}_s(\dot{z}_s - \dot{z}_{us}) \geq 0 \\ c_{min}(\dot{z}_s - \dot{z}_{us}) & \text{if } \dot{z}_s(\dot{z}_s - \dot{z}_{us}) < 0 \end{cases} \quad (3)$$

where F_{SH} is the semiactive damper force, c_{SH} is a virtual damper coefficient between the sprung mass and the sky, and c_{min} is the passive damper coefficient. The *Ground-Hook* algorithm is, Valasek et al. [1997]:

$$F_{GH} = \begin{cases} c_{GH}\dot{z}_{us} & \text{if } -\dot{z}_{us}(\dot{z}_s - \dot{z}_{us}) \geq 0 \\ c_{min}(\dot{z}_s - \dot{z}_{us}) & \text{if } -\dot{z}_{us}(\dot{z}_s - \dot{z}_{us}) < 0 \end{cases} \quad (4)$$

where F_{GH} is the semiactive damper force, and c_{GH} is a virtual damper coefficient between the unsprung mass and the ground. The hybrid controller algorithm is:

$$F_{Hybrid} = \varsigma F_{SH} + (1 - \varsigma)F_{GH} \quad (5)$$

where ς is a weighting factor to adjust for comfort or road holding, $\varsigma \in (0, 1)$.

Second, the hybrid *Mix-One-Sensor* (*M1S*), Savaresi and Spelta [2009]:

$$C_{M1S-C} = \begin{cases} C_{max} \text{ if } (\ddot{z}_s^2 - \alpha^2\dot{z}_s^2) \leq 0 \\ C_{min} \text{ if } (\ddot{z}_s^2 - \alpha^2\dot{z}_s^2) > 0 \end{cases} \quad (6)$$

$$C_{M1S-RH} = \begin{cases} C_{max} \text{ if } (\ddot{z}_s^2 - \alpha^2\dot{z}_s^2) > 0 \\ C_{min} \text{ if } (\ddot{z}_s^2 - \alpha^2\dot{z}_s^2) \leq 0 \end{cases} \quad (7)$$

where C_{M1S-C} and C_{M1S-RH} are the coefficients for comfort and road holding; $\alpha = 2\pi f$ where f is the frequency of change between passive (C_{min}) and active (C_{max}). The hybrid algorithm is the same.

Third, the *Frequency Estimation Based* (*FEB*) controller. It uses the *Root Mean Square* (*RMS*) of the deflection and deflection velocity in a time window to estimate the suspension oscillation frequency of the road. Based on this estimation the damping coefficient is adjusted, Lozoya-Santos et al. [2012].

6. RESULTS

Two types of road were used to compare the performance and feasibility of controllers in a NCS (*CAN*): a road profile and a *Boggs* type surface. The road profile simulates a rough runway surface according of standard ISO-8606:1995. The *Boggs* type surface is a sine wave with decreasing amplitude (30 - 0 mm) and increasing frequency (0.5 - 30 Hz), Boggs et al. [2006].

Since the sample time of analog inputs is 10 ms, multiple values of this were chosen: 10, 20 and 30 ms to evaluate the time delay in the network. The important time delays that should be considered in a distributed control system analysis are the sensor to controller and the controller to actuator end-to-end delays. In an *NCS*, message transmission delay can be broken into two parts: device delay and network delay. Figure 5 shows the transmission time of messages for high network traffic load with different sampling times (10 ms in top plot, 20 ms in middle plot, and 30 ms in bottom plot). Similar results correspond to low and average network traffic load. The network traffic load was generated by sending several messages into the *CAN*. The network traffic load for different sampling time were: 67.6 % with 10 ms, 32.9 % with 20 ms and 22.6 % with 30 ms

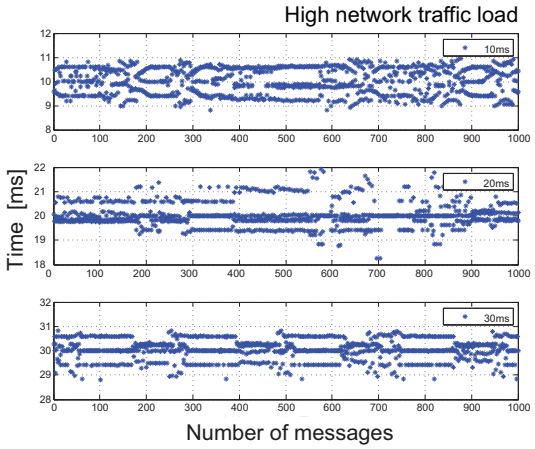

Fig. 5. Effect of different network load in the sampling time

The high available sampling time was 10 ms. Additionally, a *P2P* wired configuration was implemented as a baseline control system to compare with *CAN*-based control with a sampling frequency of 200 Hz.

Performance indices were proposed in frequency and time domain: *pseudo-Bode* diagram which allows to visualize the performance of controllers for different frequencies bandwidth and the *RMS* of the performance variables.

The comfort was evaluated by the acceleration $\ddot{z}_s$ and displacement of the sprung mass z_s, while the suspension deflection z_{def} (z_s - z_{us}) was for the road holding.

Figure 6 shows the experimental *pseudo-Bode* of acceleration and displacement of sprung mass; and also, the suspension deflection. In these figures, the tag 0 A means the softest suspension system and 2.5 A means the hardest suspension system based on the controller output. These conditions are limits for the controllers comparison. It is seen in Figs. 6(A,B) that controllers reduce acceleration and displacement response around the sprung mass resonance (1 - 2 Hz); improving the comfort. But, around the significant frequency range for road-holding (6 - 12 Hz) the gain increases considerably for all the controllers excluding the *FEB* controller, which control algorithm is designed for both comfort and road holding.

Figure 6(C) shows the deflection of unsprung mass. The controllers reduce displacement responses around the unsprung mass resonance except *M1Sc* which has a high gain in the road holding frequency ($\sim$ 10 Hz).

All controllers have a better performance than the passive damper in both frequency ranges (comfort, road holding). In the frequency range of comfort, the *FEB* controller have better performance than *M1Sc* and *SH-GHc* controllers, Figs. 6(A,B). Also, the *FEB* controller has a better performance in road holding, Figs. 6C.

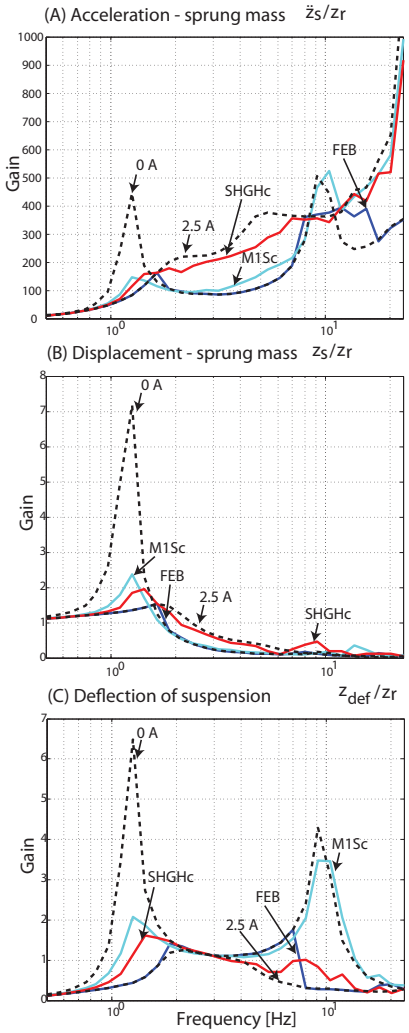

Fig. 6. Experimental Pseudo-Bodes.

Table 1 reports *RMS* values of the key variables under transient state during the road profile test. For comfort variables ($\ddot{z}_s, z_s$), the *M1Sc* controller has the best results (bold). In road holding variables (z_{def}), *FEB* is the best (bold). These results validate the experimental set up considering the *QoV* model and *ECU* into the CAN platform. To evaluate the effect of *CAN* based approach

Table 1. *RMS* values from road profile test.

Controller	$\ddot{z}_s$ $[m/s^2]$	z_s **[mm]**	z_{def} **[mm]**
FEB	0.6486	2.3253	2.3493
M1Sc	**0.3307**	**1.7433**	2.0107
SHGHc	0.5279	2.1475	**1.8141**
	M1Sc	*M1Sc*	*SHGHc*

in frequency domain, each controller was compared with its *P2P* configuration approach. The *FEB* controller has a similar behavior in both approaches for frequencies lower than 6 Hz, at higher frequencies there are variations less than 12 % for different sampling times in comfort variables, Figs. 7(A,B) and variations less than 1.8 % in road holding variables, Figs. 7C. Equivalent plots were generated for both *M1Sc* and *SH-GHc* controllers. The *M1Sc* controller has similar values for frequencies below 9 Hz, with variations less than 30 % in comfort variables and variations less than 4 % in road holding variables. The *SH-GHc* controller has greater variations, less than 28 % in comfort variables, and less than 16 % to road holding. Figure 8 shows the

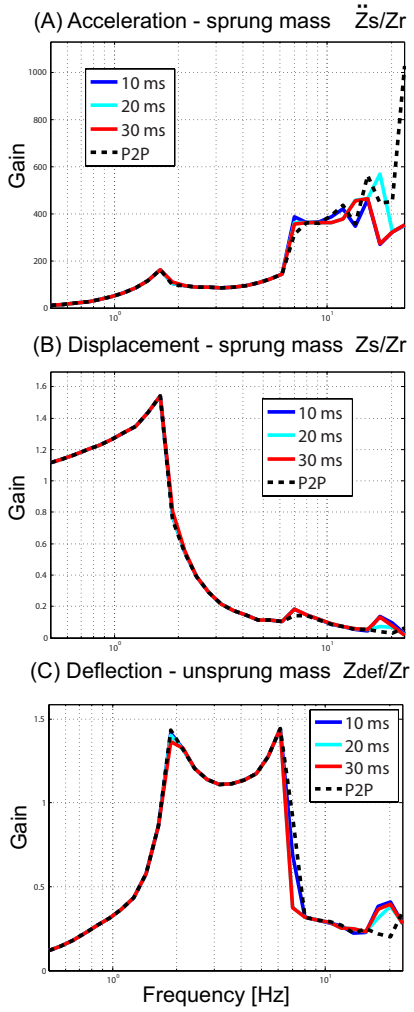

Fig. 7. Performance comparison for different sampling time, FEB controller.

RMS values of *P2P* and *CAN* based systems for different controllers and sampling times. The *RMS* of acceleration of the sprung mass shows that *M1Sc* controller has a better performance in *P2P* based system with lightly increments because the different sampling times in *CAN* based system, Fig. 8A. Based on equivalent plots for the unsprung mass displacement, the *FEB* controller presents a better performance in *P2P* based system. In suspension deflection, the *SH-GHc* controller has better performance, Fig. 8B. The results validate the expected patterns shown in Fig. 1 and the opportunity for implementing more complex algorithms in *CAN* platform.

There are some related works. Nor et al. [2012] addresses the analysis of control performance for vehicle active suspension via *CAN* based on full vehicle model. The *Linear*

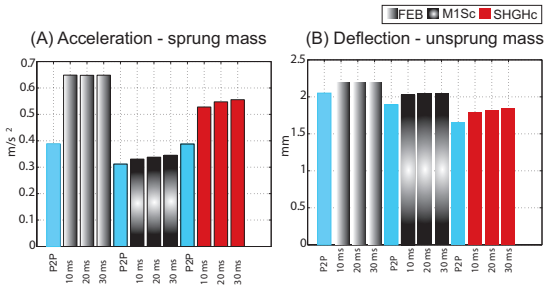

Fig. 8. *RMS* values with different sampling times.

Quadratic Regulator technique was used to reduce heave, pitch and roll variation. Various system performances were analyzed by varying *CAN* data speed, *CAN* loss probability, etc. Based on the analysis, the setup of the proposed *CAN* network for the system meet the system requirements. These authors addresses the analysis of performance for steer-by-wire system via *CAN* too, Nor et al. [2013].

Shoukry et al. [2010] applies the *Generalized Predictive Control* to a class of active suspension automotive systems. Real time *CAN*-bus Networked Embedded Control System represents the backbone of this environment. Real-Time experimental results show the efficiency controller to get a ride-comfort. Also, Sun et al. [2010] indicated that it is necessary to consider network communication quality and configuration comprehensively while design *CAN* network vehicle chassis control system. Better control algorithms that demand intense computing time will be considered for future work.

7. CONCLUSIONS

A performance analysis of automotive semi-active suspension control strategies was realized. Three *on/off* control algorithms were tested with a Quarter of Vehicle (*QoV*) model: *Sky Hook and Ground Hook* (*SH–GH*), the *hybrid Mix-One-Sensor* (*M1S*) and *Frequency Estimation Based* (*FEB*). A commercial Magneto-Rheological damper was implemented using an Artificial Neural Network approach. The automotive semi-active suspension was implemented in a commercial *CAN* based system; the control algorithms were implemented in a micro-controller system (Arduino Due) that works as *ECU* in the system.

Comfort and road holding were the main goals of semi-active suspension system. These goals were evaluated with two performance indexes: *pseudo-Bode* plots and *Root Mean Square* (*RMS*) of the key variables: acceleration and displacement of the sprung mass for comfort and deflection of the unsprung mass for road holding. Two types of road were implemented to compare the performance of controllers, a road profile and a *Boggs* type surface. Finally, a *P2P* configuration was considered in order to evaluate the sampling time in the *CAN* based system.

Results show the feasibility of this approach in commercial applications. All control algorithms have better results than the default solutions (i.e. softest or hardest suspension system). Using the *pseudo-Bode* diagrams hybrid solutions exhibit good results in both frequencies range of interest (comfort and road holding); these results were also validated with the *RMS* index .

REFERENCES

C. Boggs, L. Borg, and J. Ostanek. Efficient Test Procedures for Characterizing MR Dampers. In *ASME Int. Mechanical Eng. Congress and Exposition*, 2006.

J. Hu, G. Li, X. Yu, and S. Liu. Design and Application of SAE J1939 Communication Database in City-Bus Information Integrated Control System Development. In *Proc of the 2007 IEEE Int Conf on Mechatronics and Automation*, pages 3429–3434, China, 2007.

D. Karnopp, M.J. Crosby, and R. Harwood. Vibration Control Using Semi-Active Force Generators. *Trans. of ASME, J. of Eng. for Industry*, 96:619–626, 1974.

F.L. Lian, J.R Moyne, and D.M. Tilbury. Network Design Consideration for Distributed Control Systems. *IEEE Trans on Control Sys Tech*, 10(2):297–307, 2002.

F.L. Lian, J.R Moyne, and D.M. Tilbury. Network Protocols for Networked Control Systems. In D. Hristu-Varsakelis and W. Levine, editors, *Handbook of Networked and Embedded Control Systems*, pages 651–675. Birkhuser Boston, New York, 2005.

J.J. Lozoya-Santos, J.C. Tudon-Martinez, R. Morales-Menendez, and R.A. Ramirez-Mendoza. Comparison of On-Off Control Strategies for a Semi-Active Automotive Suspension using HiL. *IEEE Latin America Trans.*, 10 (5):2045–2052, 2012.

P.S. Marshall. A Comprehemsive Guide to Industrial Networks: Part 1. *Sensors Magazine*, 18(6), 2001.

M.B. Nor, A.R. Husainy, and A.S. Ahmad. An Analysis of CAN Performance in Active Suspension Control System for Vehicle. In *Int. CAN Conf.*, pages 12–19, 2012.

M.B. Nor, A.R. Husainy, and A.S. Ahmad. An Analysis of CAN-based Steer-by-Wire System Performance in Vehicle. In *2013 IEEE Int Conf on Control System, Computing and Eng*, pages 350–355, 2013.

R. Bosch GmbH. *CAN specification version 2.0*. Stuttgart, Germany, 1991.

SAE. Surface Vehicle Recommended Practice, SAE J1939. Technical report, SAE, 2005.

V. Sankaranarayanan, M.E. Emekli, B.A. Gilvenc, L. Guvenc, E.S. Ozturk, E.S. Ersolmaz, I.E. Eyol, and M. Sinal. Semiactive Suspension Control of a Light Commercial Vehicle. *IEEE/ASME Trans. on Mechatronics*, 13(5):598–604, 2008.

S.M. Savaresi and C. Spelta. A Single-Sensor Control Strategy for Semi-Active Suspensions. *IEEE Trans. on Control Systems Technology*, 17(1):143 – 152, 2009.

Y. Shoukry, M. El-Shafie, and S. Hammad. Networked Embedded Generalized Predictive Controller for an Active Suspension System. In *American Control Conf*, pages 4570–4575, 2010.

N. Sun, Y. Wan, and Z. Guo. Modeling of Distributed Network Control for Vehicle Stability Based on True-Time. In *Int Conf on E-Product E-Service and E-Entertainment*, pages 1–4, 2010.

M. Valasek, M. Novak, Z. Sika, and O. Vaculin. Extended Ground-Hook – New Concept of Semi-Active Control of Truck Suspension. *Vehicle Syst. Dyn.*, 29:289–303, 1997.

R. Vargas-Rodriguez and R. Morales-Menendez. Network-Induced Delay Models for CAN-based Networked Control Systems. In 7^{th} *IFAC Int Conf on Fieldbuses and Networks in Ind and Embedded*, volume 7, pages 85–92, 2007.